

## Supporting information

### One-pot synthesis of porous Ag@Pt core-shell cocatalysts on g-C<sub>3</sub>N<sub>4</sub> for enhanced photocatalytic H<sub>2</sub> production from lignocellulose reforming

Wenchang Li<sup>a</sup>, Weiwu Chen<sup>b</sup>, Jianzhong Guo<sup>a\*</sup>, Chunzheng Wu<sup>a\*</sup>

<sup>a</sup> College of Chemistry and Materials Engineering, Zhejiang A&F University, Hangzhou 311300, P. R. China.

<sup>b</sup> Yangtze Delta Region Institute (Huzhou), University of Electronic Science and Technology of China, Huzhou, 313001, PR China.

\* Corresponding authors: guojianzhong@zafu.edu.cn (J. Guo) and wucz@zafu.edu.cn (C. Wu)

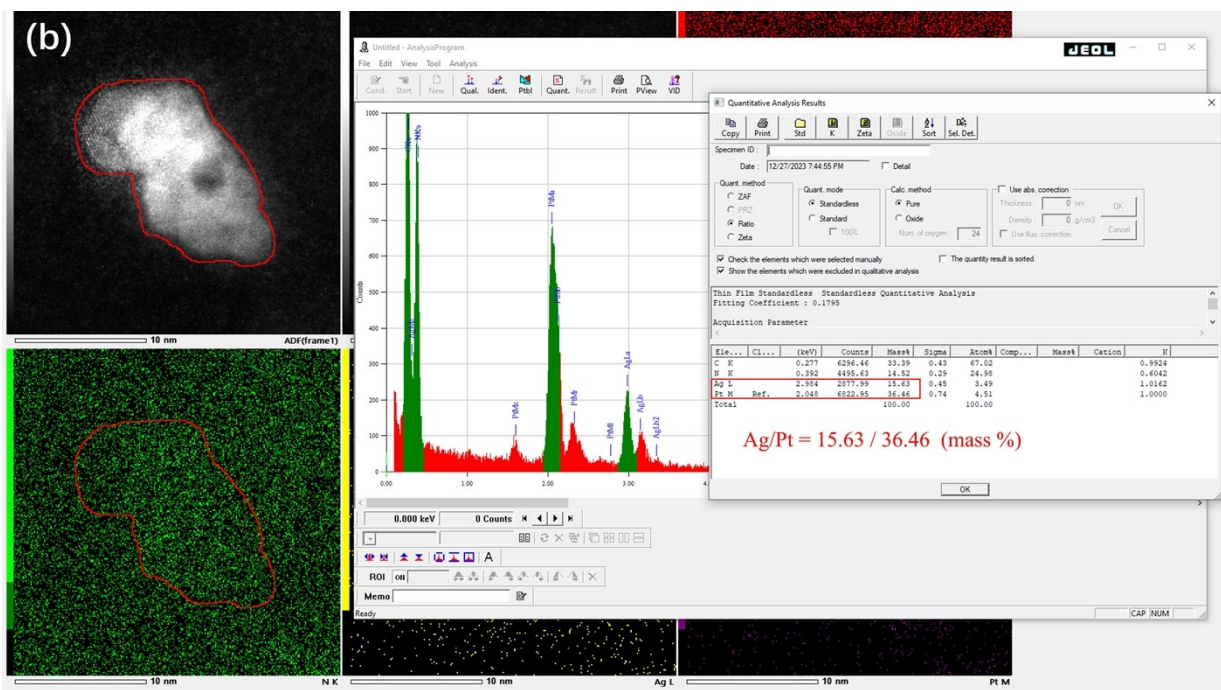
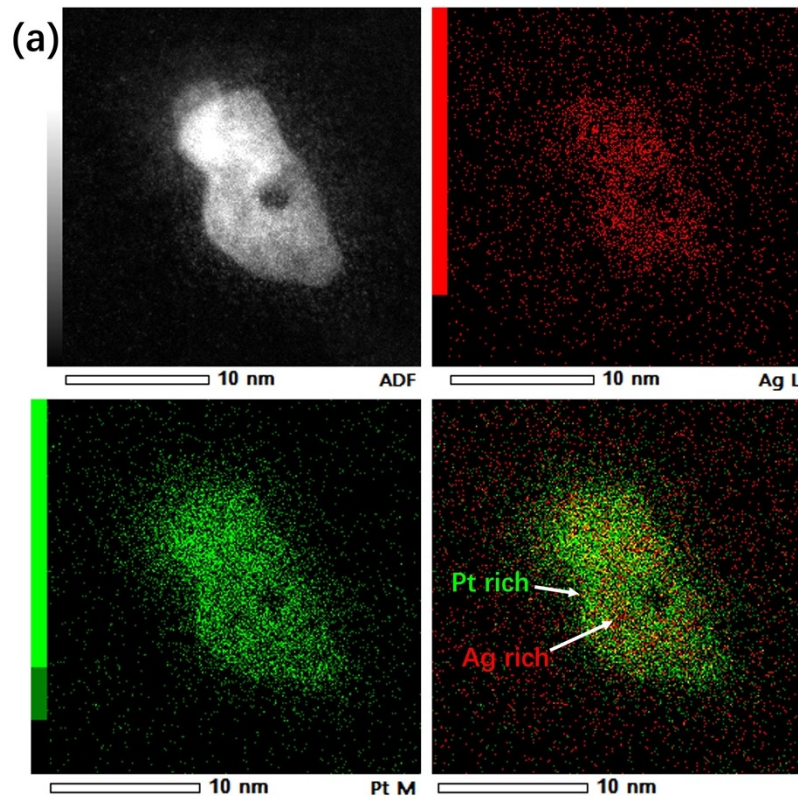


**Figure S1.** (a) EDS mapping of  $\text{Ag}_1\text{Pt}_3/\text{CN}$ , and (b) the corresponding metal ratio analysis.

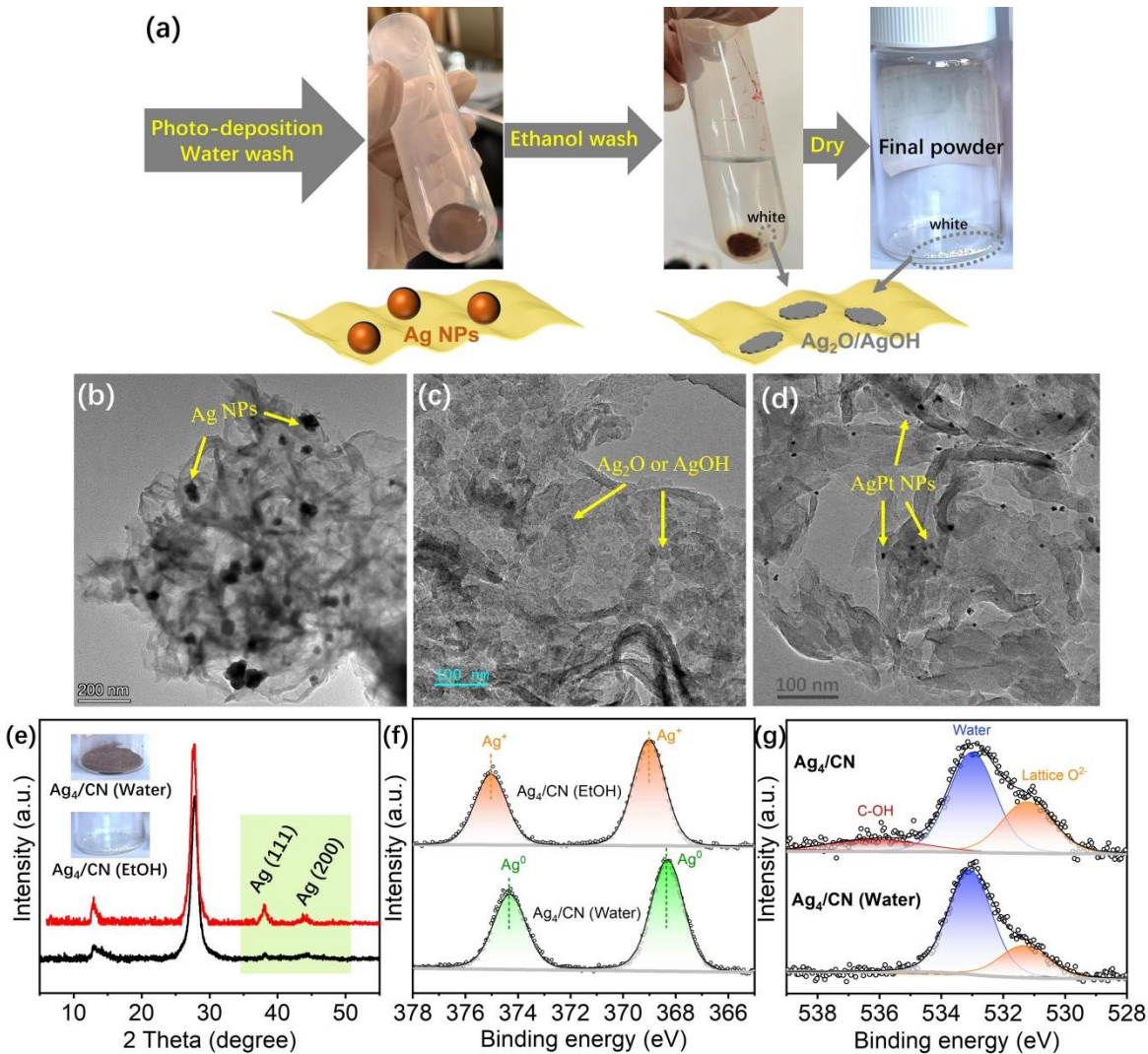


**Figure S2.** (a) Scheme illustrates the transformation of Ag NPs when washed with ethanol. TEM images of (b) water-washed  $\text{Ag}_4/\text{CN}$ , (c) ethanol-washed  $\text{Ag}_4/\text{CN}$ , and (d) ethanol-washed  $\text{Ag}_1\text{Pt}_3/\text{CN}$ . (e) The XRD patterns of water-washed  $\text{Ag}_4/\text{CN}$  and ethanol-washed  $\text{Ag}_4/\text{CN}$ . (f) XPS Ag3d and (g) XPS O1s spectra of water-washed  $\text{Ag}_4/\text{CN}$  and ethanol-washed  $\text{Ag}_4/\text{CN}$ .

### Calculation of reduction potentials:

(1) Since  $\text{Ag}^+$  ions cannot exist in an alkaline solution, we refer to the standard reduction potential for the  $\text{Ag}_2\text{O}/\text{Ag}$  pair, which is 0.342 V. The standard reduction potential for the  $\text{Pt}(\text{OH})_6^{2-}/\text{Pt}$  pair is not known, but it can be approximated using the  $\text{PtCl}_6^{2-}/\text{Pt}$  pair, which is calculated to be 0.718 V, based on the  $\text{PtCl}_6^{2-}/\text{PtCl}_4^{2-}$  (0.68 V) and  $\text{PtCl}_4^{2-}/\text{Pt}$  (0.755 V) pairs:

$$\varphi^\theta(\text{PtCl}_6^{2-}/\text{Pt}) \times 4 = \varphi^\theta(\text{PtCl}_6^{2-}/\text{PtCl}_4^{2-}) \times 2 + \varphi^\theta(\text{PtCl}_4^{2-}/\text{Pt}) \times 2$$

$$\varphi^\theta(\text{PtCl}_6^{2-}/\text{Pt}) = \frac{0.68 + 0.755}{2} = 0.718 \text{ V}$$

(2) According to the Nernst equation at 298 K, the concentrations of  $\text{Pt}(\text{OH})_6^{2-}$  and  $\text{OH}^-$  could influence the reduction potentials (refer to detailed calculations below), resulting in adjusted values of 0.617 V for  $\text{Pt}(\text{OH})_6^{2-}/\text{Pt}$  and 0.314 V for  $\text{Ag}_2\text{O}/\text{Ag}$  at the initial state. This suggests that galvanic replacement between  $\text{Pt}(\text{OH})_6^{2-}$  and  $\text{Ag}$  is feasible.

For the  $\text{Pt}(\text{OH})_6^{2-} + 4\text{e}^- = \text{Pt} + 6\text{OH}^-$  reaction, assuming that the standard reduction potential was close to the  $\text{PtCl}_6^{2-}/\text{Pt}$  pair, then the actual reduction potential of the  $\text{Pt}(\text{OH})_6^{2-}/\text{Pt}$  pair at the initial state is calculated to be 0.617 V:

$$\varphi(\text{Pt}(\text{OH})_6^{2-}/\text{Pt}) = \varphi^\theta(\text{Pt}(\text{OH})_6^{2-}/\text{Pt}) + \frac{0.059}{4} \lg \frac{c(\text{Pt}(\text{OH})_6^{2-})}{c^6(\text{OH}^-)} \approx 0.718 + \frac{0.059}{4} \lg \frac{1.03 \times 10^{-4}}{3^6} = 0.617 \text{ V}$$

For the  $\text{Ag}_2\text{O} + \text{H}_2\text{O} + 2\text{e}^- = 2\text{Ag} + 2\text{OH}^-$  reaction, the actual reduction potential of the  $\text{Ag}_2\text{O}/\text{Ag}$  pair is calculated to be 0.314 V:

$$\varphi(\text{Ag}_2\text{O}/\text{Ag}) = \varphi^\theta(\text{Ag}_2\text{O}/\text{Ag}) + \frac{0.059}{2} \lg \frac{1}{c^2(\text{OH}^-)}$$

$$\approx 0.342 + \frac{0.059}{2} \lg \frac{1}{3^2} = 0.314 \text{ V}$$

(3) In principle, the galvanic replacement reaction would stop when  $\varphi(\text{Pt}(\text{OH})_6^{2-}/\text{Pt}) = \varphi(\text{Ag}_2\text{O}/\text{Ag})$ .

Assuming that the concentration of  $\text{OH}^-$  did not change (NaOH is excessive), the final concentration of  $\text{Pt}(\text{OH})_6^{2-}$  was calculated to be  $2.97 \times 10^{-15}$  mol/L, indicating that ~100% of  $\text{Pt}(\text{OH})_6^{2-}$  would be reacted.

$$\varphi(\text{Pt}(\text{OH})_6^{2-}/\text{Pt}) = \varphi(\text{Ag}_2\text{O}/\text{Ag})$$

$$0.718 + \frac{0.059}{4} \lg \frac{c(\text{Pt}(\text{OH})_6^{2-})}{3^6} = 0.314$$

$$c\big(Pt(OH)_6^{2-}\big)=2.97\times10^{-15}\,mol/L$$

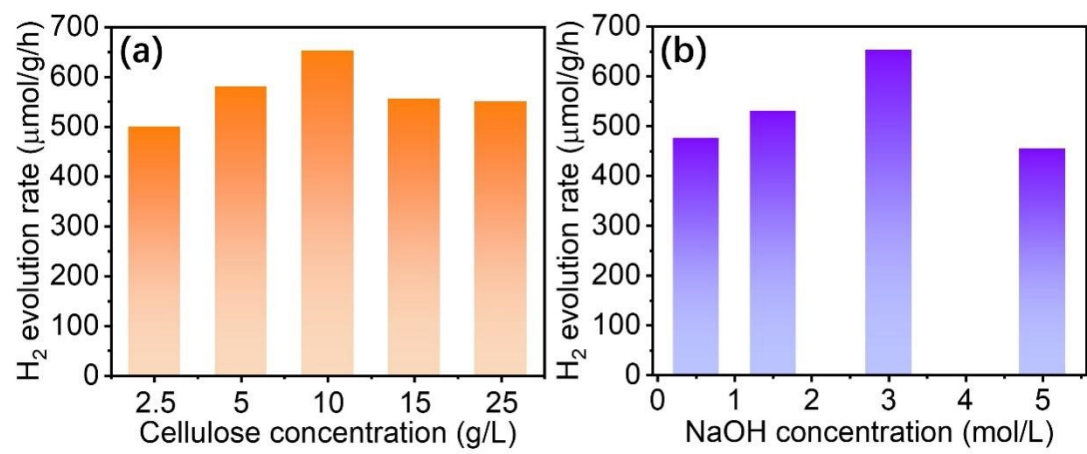


**Figure S3.** the effects of (a) cellulose concentration and (b) NaOH concentration on  $\text{H}_2$  evolution.

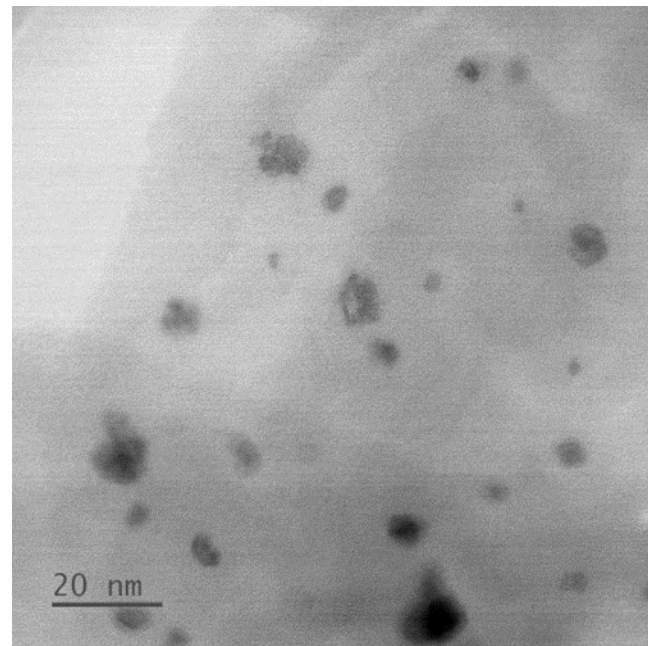


**Figure S4.** TEM image of  $\text{Ag}_1\text{Pt}_3/\text{CN}$  after 12 hours of test.

**Table S1.** Comparison of our Ag<sub>1</sub>Pt<sub>3</sub>/CN with the reported g-C<sub>3</sub>N<sub>4</sub> and TiO<sub>2</sub> based photocatalysts in H<sub>2</sub> evolution from cellulose reforming.

Photocatalyst	HER rate (μmol/g/h)	Light source	Conditions	Reference
Ag <sub>1</sub> Pt <sub>3</sub> /CN (10 mg)	652.7	300 W Xe lamp 150 mW/cm <sup>2</sup>	5 g/L cellulose 3 M NaOH	This work
0.21 wt.% Pt/C <sub>3</sub> N <sub>4</sub> (10 mg)	1110	40 W blue LED (λ = 427 nm)	2 g/L α-cellulose 10 M NaOH	Wang et al. <sup>[1]</sup>
Pt <sub>1</sub> Au <sub>3</sub> /CN (10 mg)	1186	300 W Xe lamp 150 mW/cm <sup>2</sup>	5 g/L cellulose 3 M NaOH	Ding et al. <sup>[2]</sup>
4 wt.% Pt/ <sup>NCN</sup> CN <sub>x</sub> (5 mg)	~ 10	AM1.5G	33.3 g/L cellulose 10 M KOH	Kasap et al. <sup>[3]</sup>
0.8 wt.% Pt/HCN-NEA (30 mg)	1007	Xe lamp (λ > 420 nm)	2.5 g/L α-cellulose 5 M NaOH	Liu et al. <sup>[4]</sup>
1 wt.% Pt/monolayer g-C <sub>3</sub> N <sub>4</sub> (50 mg)	72.67	300 W Xe lamp (λ > 420 nm)	5 g/L α-cellulose pH = 10	Rao et al. <sup>[5]</sup>
2 wt.% Pt/CNNs (50 mg)	94.33	300 W Xe lamp (400 < λ < 780nm)	0.5 g/L cellulose 3 M NaOH	Hong et al. <sup>[6]</sup>
3 wt.% Pt/K-PHI-450 (200 mg)	190.6	420 < λ < 800nm	50 g/L cellulose 0.8 M NaOH	Nimbalkar et al. <sup>[7]</sup>
g-C <sub>3</sub> N <sub>4</sub> -C <sub>0.40</sub> (20 mg)	104.4	300 W Xe lamp (λ ≥ 630 nm)	20 g/L α-cellulose 10 M NaOH	Xie et al. <sup>[8]</sup>
0.3 wt.% Pd/TiO <sub>2</sub> (50 mg)	436	3 MH-lamps of 150 W	3.33 g/L cotton linter cellulose	Abdul Razak et al. <sup>[9]</sup>
1% wt.% Pt/anatase TiO <sub>2</sub> nanosheet (100 mg)	275	300 W Xe lamp	4 g/L cellulose Sonication	Cheng et al. <sup>[10]</sup>
2 wt.% Pt/P25 (10 mg)	614.7	395 nm LED	5 g/L Napkin 10 M NaOH	Wu et al. <sup>[11]</sup>
TiO <sub>2</sub> /NiO <sub>x</sub> @C <sub>g</sub> (20 mg)	270	500 W Xe lamp	20 g/L cellulose Sonication	Zhang et al. <sup>[12]</sup>
1 wt.% Pt/TiO <sub>2</sub> (100 mg)	305.83	300 W Xe lamp	5 mL filtrate of acid treated corn straw	Zhou et al. <sup>[13]</sup>

## Reference

- [1] Wang, E.; Mahmood, A.; Chen, S.-G.; Sun, W.; Muhammed, T.; Yang, X.; Chen, Z., Solar-Driven Photocatalytic Reforming of Lignocellulose into H<sub>2</sub> and Value-Added Biochemicals. *ACS Catalysis* **2022**, *12*, 11206-11215.
- [2] Ding, F.; Yu, H.; Tu, R.; Li, S.; Chen, L.; Li, B.; Guo, J.; Wu, C., Engineering Au-Pt atomic alloy cocatalysts for enhanced H<sub>2</sub> production from photo-reforming of lignocellulosic biomass wastes. *Chemical Engineering Journal* **2024**, *496*, 154260.
- [3] Kasap, H.; Achilleos, D. S.; Huang, A.; Reisner, E., Photoreforming of Lignocellulose into H<sub>2</sub> Using Nanoengineered Carbon Nitride under Benign Conditions. *Journal of the American Chemical Society* **2018**, *140*, 11604-11607.
- [4] Liu, Q.; Wang, F.; Jiang, Y.; Chen, W.; Zou, R.; Ma, J.; Zhong, L.; Peng, X., Efficient photoreforming of lignocellulose into H<sub>2</sub> and photocatalytic CO<sub>2</sub> reduction via in-plane surface dyadic heterostructure of porous polymeric carbon nitride. *Carbon* **2020**, *170*, 199-212.
- [5] Rao, C.; Xie, M.; Liu, S.; Chen, R.; Su, H.; Zhou, L.; Pang, Y.; Lou, H.; Qiu, X., Visible Light-Driven Reforming of Lignocellulose into H<sub>2</sub> by Intrinsic Monolayer Carbon Nitride. *ACS Applied Materials & Interfaces* **2021**, *13*, 44243-44253.
- [6] Hong, Y.; Zhang, X.; Lin, X.; Liu, E.; Wang, L.; Shi, W.; Duan, X., Ultrathin 2D g-C<sub>3</sub>N<sub>4</sub> nanosheets for visible-light photocatalytic reforming of cellulose into H<sub>2</sub> under neutral conditions. *Journal of Chemical Technology & Biotechnology* **2022**, *97*, 1717-1725.
- [7] Nimbalkar, D. B.; Nguyen, V.-C.; Shih, C.-Y.; Teng, H., Melem-derived poly(heptazine imide) for effective charge transport and photocatalytic reforming of cellulose into H<sub>2</sub> and biochemicals under visible light. *Applied Catalysis B: Environmental* **2022**, *316*, 121601.
- [8] Xie, Z.-K.; Jia, Y.-J.; Huang, Y.-Y.; Xu, D.-B.; Wu, X.-J.; Chen, M.; Shi, W.-D., Near-Infrared Light-Driven Photocatalytic Reforming Lignocellulose into H<sub>2</sub> and Chemicals over Heterogeneous Carbon Nitride. *ACS Catalysis* **2023**, *13*, 13768-13776.
- [9] Abdul Razak, S.; Mahadi, A. H.; Abdullah, R.; Yasin, H. M.; Ja'afar, F.; Abdul Rahman, N.; Bahruji, H., Biohydrogen production from photodecomposition of various cellulosic biomass wastes using metal-TiO<sub>2</sub> catalysts. *Biomass Conversion and Biorefinery* **2023**, *13*, 8701-8712.
- [10] Cheng, Q.; Yuan, Y.-J.; Tang, R.; Liu, Q.-Y.; Bao, L.; Wang, P.; Zhong, J.; Zhao, Z.; Yu, Z.-T.; Zou, Z., Rapid Hydroxyl Radical Generation on (001)-Facet-Exposed Ultrathin Anatase TiO<sub>2</sub> Nanosheets for Enhanced Photocatalytic Lignocellulose-to-H<sub>2</sub> Conversion. *ACS Catalysis* **2022**, *12*, 2118-2125.
- [11] Wu, C.; Fang, L.; Ding, F.; Mao, G.; Huang, X.; Lu, S., Photocatalytic hydrogen production from water and wastepaper on Pt/TiO<sub>2</sub> composites. *Chemical Physics Letters* **2023**, *826*, 140650.
- [12] Zhang, L.; Wang, W.; Zeng, S.; Su, Y.; Hao, H., Enhanced H<sub>2</sub> evolution from photocatalytic cellulose conversion based on graphitic carbon layers on TiO<sub>2</sub>/NiO<sub>x</sub>. *Green Chemistry* **2018**, *20*, 3008-3013.
- [13] Zhou, Y.; Lin, D.; Ye, X.; Sun, B., Reuse of Acid-treated Waste Corn Straw for Photocatalytic Hydrogen Production. *ChemistrySelect* **2022**, *7*, e202201596.